



Full Length Article

Recyclable CuS sorbent with large mercury adsorption capacity in the presence of SO₂ from non-ferrous metal smelting flue gas

Wei Liu^a, Haomiao Xu^{a,b}, Yong Liao^a, Zongwen Quan^a, Sichao Li^a, Songjian Zhao^a, Zan Qu^a, Naiqiang Yan^{a,*}

^a School of Environmental Science and Engineering, Shanghai Jiao Tong University, Shanghai 200240, China

^b Shanghai Institute of Pollution Control and Ecological Security, Shanghai 200092, China



ARTICLE INFO

Keywords:

Elemental mercury
Non-ferrous metal smelting flue gas
Metal sulfide
SO₃

ABSTRACT

Gaseous elemental mercury (Hg⁰) is difficult to dispose using traditional sorbents when co-existed with high concentration of SO₂ from non-ferrous smelting gas. CuS was selected for Hg⁰ removal from non-ferrous metal smelting flue gas due to large Hg⁰ uptake capacity under SO₂ condition. Hg⁰ removal experiments indicated that CuS has the largest Hg⁰ adsorption capacity compared to that of ZnS, CdS, MnS and SnS. The Hg⁰ adsorption rate and capacity of CuS at 50 °C was 0.0716 mg/(g·min) and 50.17 mg/g with 50% breakthrough threshold, respectively. In addition, the effects of reaction factors such as reaction temperatures and gas components (O₂, SO₂, H₂O, SO₃) on Hg⁰ removal performances were investigated. O₂, H₂O and SO₂ showed negligible influences on Hg⁰ capture. However, SO₃ competed with mercury for adsorption sites, resulting in a decrease of mercury adsorption capacity. The XPS analysis and Hg-TPD results indicated that the adsorbed mercury mainly existed as HgS on the material surface. CuS exhibited high mercury adsorption capacity under SO₂ atmosphere at low temperature, appeared to be a promising material for Hg⁰ capture from non-ferrous metal smelting flue gas. They can be used co-benefit with electrostatic demister (ESD), upstream entering the acid plant for SO₂ recovery.

1. Introduction

Mercury is one of the most hazardous global pollutants due to its high toxicity, long-rang atmospheric transportation and bio-accumulation performance [1]. After decades of negotiations, the *Intergovernmental Negotiating Committee (INC)* had adopted the *Minamata Convention on Mercury* in January 2013, aiming at controlling anthropogenic mercury emissions globally [2]. And this convention had come into force on August 16, 2017. Previous researches indicated that mercury emission from nonferrous metal smelters accounted for approximately 27.6% of the total in China, particularly in zinc, copper, lead and industrial gold production processes [3–6]. Therefore, it is significant to control mercury emission from non-ferrous metal smelters.

Generally, mercury is released from sulfides ores to flue gases during the pyrometallurgical processes of non-ferrous metals, and primarily exists in three forms: elemental mercury (Hg⁰), oxidized mercury (Hg²⁺) and particle-associated mercury (Hg_p) [7]. Generally speaking, gaseous mercury is primarily coexisted with high concentration SO₂ and SO₃ in flue gas. Before entering the acid plant, acid mist/SO₃ and particles are removed for avoiding V₂O₅ catalyst poisoning in a series of air pollution control devices (APCDs) including

cyclone (CC), electrostatic precipitator (ESP), wet flue gas scrubber (WFGS) and electrostatic demister (ESD). Using these APCDs can achieve a co-benefit removal of mercury. For example, most of Hg_p can be simultaneously collected by CC or ESP. Hg²⁺ can be captured by WFGS or ESD due to its high solubility in water and sulfuric. However, it is difficult to effectively remove Hg⁰ by APCDs due to its highly volatility and insolubility [8]. Therefore, to meet the strict regulation for mercury emissions, it requires additional Hg⁰ removal techniques after the purification system.

Currently, the control methods for Hg⁰ emissions from non-ferrous metal smelters mainly contains two categories: the one is adsorption technique which first oxidize Hg⁰ with strong oxidants and then remove oxidized mercury, or to capture Hg⁰ with specific adsorbents [9]. Another one is absorption technique, such as the Boliden–Norzink and Bolchem processes. Absorption technique is limited for widely application due to high operation cost, serious corrosion and potential environmental risk [10]. Meanwhile, various types of sorbents, such as activated carbon, selenium, have been used for the adsorption of mercury [11]. However, most of these sorbents are not suitable for usage due to low mercury capacities. Some chemicals such as sulfur, halogen, and noble metals were applied for the modification of sorbents [12–15].

* Corresponding author.

E-mail address: nqyan@sjtu.edu.cn (N. Yan).

<https://doi.org/10.1016/j.fuel.2018.08.062>

Received 20 May 2018; Received in revised form 18 July 2018; Accepted 13 August 2018

Available online 27 August 2018

0016-2361/ © 2018 Published by Elsevier Ltd.

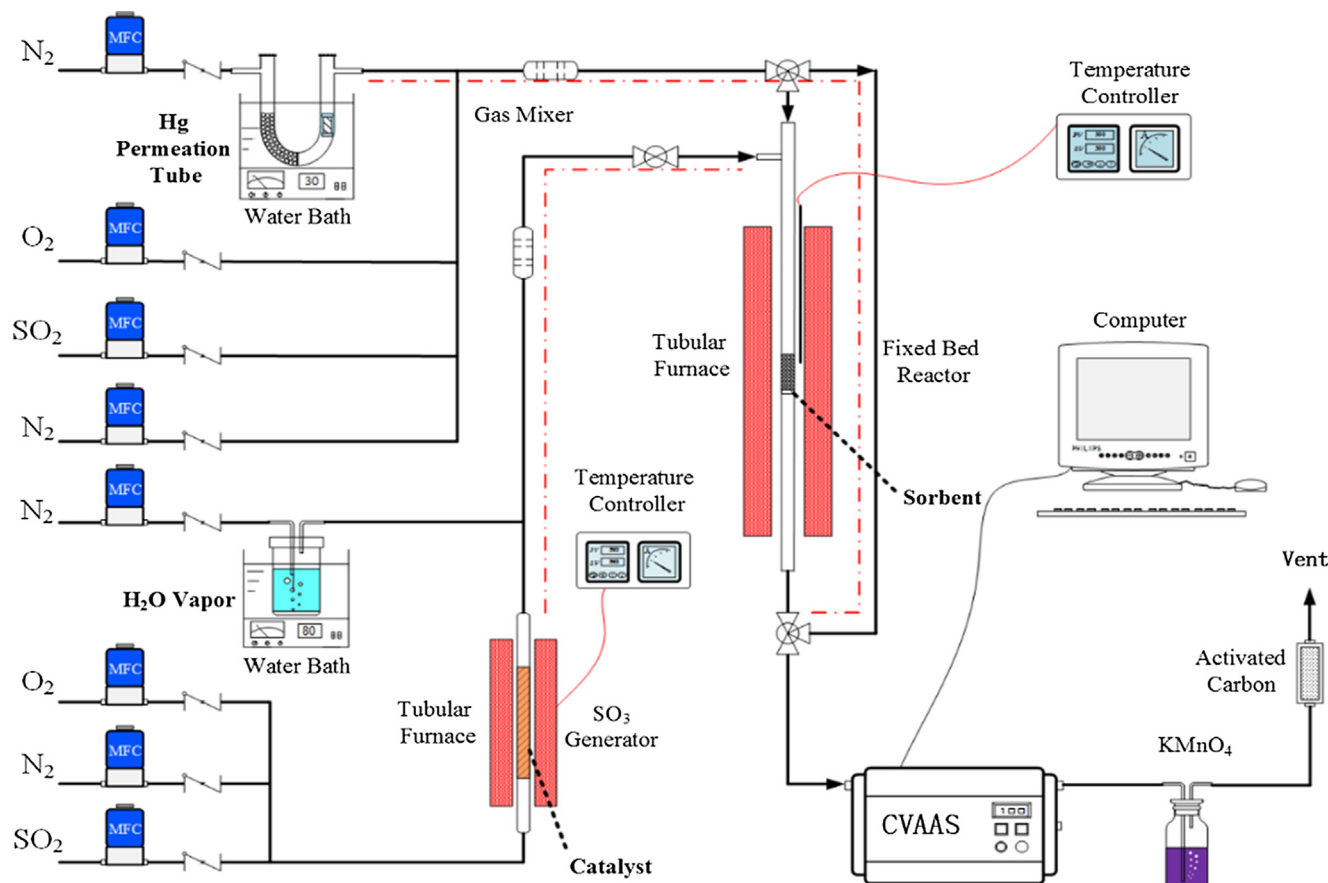


Fig. 1. Schematic diagram of lab-scale Hg^0 adsorption evaluate system.

Although mercury adsorption capacities were enlarged, most of them were easily suffered from the poisons of H_2O and SO_2 [16]. Therefore, developing novel sorbents to remove Hg^0 in flue gas containing high concentration SO_2 is important.

Chemical functionalization by sulfur is an important method to enlarge mercury adsorption capacity, resulting from the fact that surface sulfur compounds provide sufficient binding sites for mercury, forming stable mercuric sulfides (HgS) [14,17]. Metal sulfides are treated as promising adsorbents for Hg^0 due to its extensive active sulfur sites, low cost and environmental friendliness. Compared with some traditional sorbents, metal sulfides exhibit excellent Hg^0 capture performances and super resistances to H_2O and SO_2 . Li et al. prepared nano-ZnS with a huge surface area, which exhibited a superior mercury adsorption capacity ($497.84 \mu\text{g/g}$) than that of commercial activated carbons [18,19]. Liao et al. chose magnetic pyrrhotite as a recyclable sorbent to remove Hg^0 from the flue gas because of the excellent resistance of H_2O and SO_2 at low temperature [20]. However, mercury adsorption capacities of these metal sulfides are still too low to use in real industrial applications. Therefore, developing metal sulfides sorbents with larger mercury adsorption capacity is the key for controlling mercury emission from nonferrous metals smelting.

Copper sulfides (CuS) has been widely investigated for its potential application in Li-ion rechargeable batteries, gas sensors, photovoltaic devices, and catalysis. CuS composed abundant active sulfur sites is promising to remove Hg^0 effectively. In addition, literatures indicated that Cu-terminated active sites have strong adsorption performance for mercury [21]. Moreover, CuS is a cheap raw material in non-ferrous metal melting industry. Taking these advantages into account, we consider that using CuS to remove Hg^0 in smelting off-gas may be a scientifically sound and economically feasible technique.

In this study, CuS was prepared by precipitation method to remove

Hg^0 in non-ferrous metal smelting flue gas. The influences of flue gas components such as O_2 , SO_2 , H_2O and SO_3 on mercury adsorption performances, were investigated in a fixed-bed reactor. The potential application of CuS accompany with WFGS and EDS systems was discussed. Additionally, the mechanism for Hg^0 adsorption was also investigated.

2. Experimental section

2.1. Preparation of materials

Sodium sulphide ($\text{Na}_2\text{S}\cdot 9\text{H}_2\text{O}$) was purchased from Shanghai Macklin Biochemical Company. Zinc nitrate ($\text{Zn}(\text{NO}_3)_2\cdot 6\text{H}_2\text{O}$), manganese nitrate ($\text{Mn}(\text{NO}_3)_2\cdot x\text{H}_2\text{O}$), tin chloride ($\text{SnCl}_2\cdot 2\text{H}_2\text{O}$), cadmium chloride (CdCl_2), copper nitrate ($\text{Cu}(\text{NO}_3)_2\cdot 3\text{H}_2\text{O}$) were purchased from Sinopharm Chemical Reagent Company. All reagents were used as received without further purification. All the chemicals were of AR grade. Distilled water used for all dilutions and sample preparations.

Synthesis of metal sulfide. Metal sulfide sorbents were synthesized using simple precipitation method. In a typical procedure, 1 M aqueous solution of metal nitrates ($\text{Cu}(\text{NO}_3)_2\cdot 3\text{H}_2\text{O}$, $\text{Zn}(\text{NO}_3)_2\cdot 6\text{H}_2\text{O}$, $\text{Mn}(\text{NO}_3)_2\cdot x\text{H}_2\text{O}$ etc.) and 1 M aqueous solution of Na_2S were prepared using distilled water. Then Na_2S solution was added dropwise to the metal nitrates solution under vigorous stirring for 2 h at room temperature. The resulting turbid dispersion was aged for 2 h. The products were separated from the solution by centrifugation. Then, the samples were washed several times with distilled water and centrifuged, dried under vacuum at 65°C for 12 h. Finally, the collected samples were ground and sieved through 120/180 meshes before used in Hg^0 removal tests.

2.2. Characterization of materials

The Brunauer-Emmett-Teller (BET) surface area and average pore size tests of sorbents were determined by N₂ adsorption at −196 °C using a quartz tube (Quanta chrome 2200 e). Prior to measurement, the sorbents were degassed at 110 °C for 2 h. Powder X-ray diffraction (XRD) patterns were carried out on Shimadzu XRD-6100 diffractometer with Cu-Kα radiation (40 kV and 40 mA). The data were recorded at a scan rate of 10 deg/min in the 2θ range from 10 to 80°. X-ray photoelectron spectroscopy (XPS) measurements were performed on an Ultra DLD (Shimadzu-Kratos) spectrometer with Al Kα as the excitation source, and the C 1s line at 284.6 eV was used as a reference for the binding energy calibration. Temperature programmed desorption (TPD) experiments were carried out on a self-made mercury adsorption performance evaluation device.

2.3. Measurement of Hg⁰ adsorption performance

To evaluate the mercury adsorption performance of as-synthesized sorbents, we established a lab-scale fixed-bed adsorption system as shown in Fig. 1, which includes mercury generation system, humidification system, SO₃ generation system, fixed bed reactor system, mercury detection system, exhaust gas treatment system and gas flow control system. The concentration of Hg⁰ was maintained at about 1300 μg/m³ by adjusting the N₂ flow rate to pass through the mercury permeation tube and the temperature of water bath. SO₃ was generated by means of SO₂ passing through a heated catalyst bed. Hg⁰ concentration of off-gas was recorded by a cold vapor atomic absorption spectrometer mercury detector (CVASS), which was adjusted by Lumex RA 915+. Hg⁰ capture experiments were carried out using a quartz tube with internal diameter of 6 mm in fixed bed reactor. 10 mg of prepared sorbents were used for all tests with a total gas flow rate of 800 mL/min.

Table 1 provided a summary of the experimental reaction conditions. Experiment set I was designed to investigate the Hg⁰ removal efficiencies over different sulfides. And set II was aimed at investing the optimum reaction temperature for Hg⁰ capture. Set III was conducted to investigate the effect of space velocity on Hg⁰ removal efficiency. All the experiments were carried out under 5% O₂. In set IV–VIII, the effect of flue gas components (O₂, SO₂, H₂O, SO₃) on Hg⁰ removal were studied. Set IX was aimed at identifying the mercury species and explaining the mechanism of Hg⁰ removal over CuS by Hg-TPD.

The area under the inlet Hg⁰ concentration line and above a breakthrough curves, corresponding to Hg⁰ on the prepared sorbents during 180 min, was used to calculate the mercury adsorption capacity of the sorbents. The mercury breakthrough ratio (η) and adsorption capacity (Q) were used to evaluate the Hg⁰ adsorption performance of the sorbents according to Eqs. (1) and (2):

Table 1
Experimental reaction conditions.

Experiment	Flue gas components	Temperature (°C)	Sorbents
Set I	5% O ₂	50	Different metal sulfides
Set II	5% O ₂	25–175	CuS
Set III	5% O ₂ , with different space velocity	50	CuS
Set IV	0–10% O ₂	50	CuS
Set V	5% O ₂ , 0–5000 ppm SO ₂	50	CuS
Set VI	5% O ₂ , 0–10% H ₂ O	50	CuS
Set VII	5% O ₂ , 10% H ₂ O, 1000 ppm SO ₂ (SFG)	50	CuS
Set VIII	5% O ₂ , sorbents were pretreated with SO ₃	50	CuS
Set IX	N ₂ , sorbents were pretreated with SO ₃	25–700	CuS

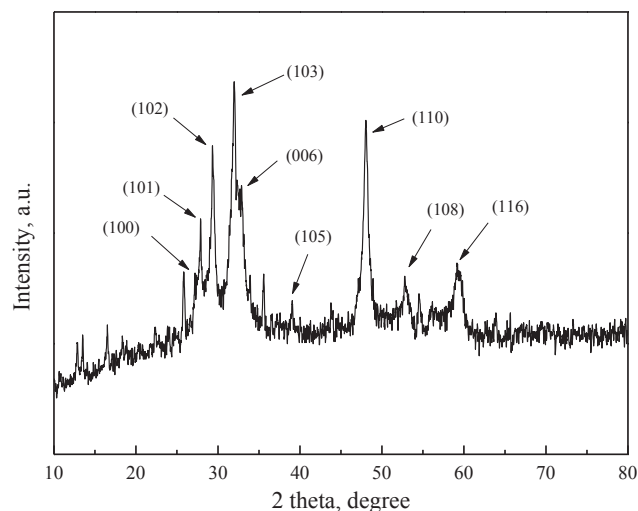


Fig. 2. XRD pattern of CuS.

$$\eta = \frac{C_o}{C_i} \times 100\% \quad (1)$$

$$Q = \frac{1}{m} \int_{t_1}^{t_2} (C_i - C_o) \times f \times dt \quad (2)$$

where Q is the Hg⁰ adsorption capacity (mg/g), C_i and C_o represent the inlet and outlet Hg⁰ concentration (μg/m³), respectively. m is the mass of sorbent (g), f denotes the flow rate of the influent, and t is the adsorption time (min). It is obvious that the smaller value of the ratio (η) indicates a higher mercury removal efficiency.

3. Results and discussion

3.1. Characterization of as-prepared composites

XRD pattern of CuS is shown in Fig. 2. All the peaks in XRD pattern of CuS were indexed to covellite, the hexagonal phase of CuS (JCPDS Card No. 06-0464, a = 3.792 Å and c = 16.34 Å) [22]. The strong and sharp diffraction peaks suggested that the as-obtained products were well crystalline. The average size of particles for CuS calculated by using the Scherrer formula with all the reflection peaks was 43 nm. As shown in Table 3, the specific surface area of CuS was 31.129 m²/g.

Table 2
Comparative summary of low-temperature mercury sorbents.

Sorbents	Adsorption capacity (mg/g)	Reaction rate (mg/(g·min))	Gas condition	Temperature (°C)
CuS (this paper)	50.17 (50%)	0.0716	5% O ₂ 1300 μg/m ³ Hg ⁰	50
[MoS ₄] ²⁻ /CoFe-LDH [26]	16.39	–	4% O ₂ 350 μg/m ³ Hg ⁰	75
H ₂ S-Modified Fe-Ti Spinel [14]	0.69 (5%)	0.00192	110 μg/m ³ Hg ⁰	60
Pyrrhotite [20]	0.22 (4%)	0.00028	5% O ₂ 120 μg/m ³ Hg ⁰	60
Fe _{0.1} Zn _{0.9} S [32]	8.65 (47%)	0.00482	Air 1600 μg/m ³ Hg ⁰	20
Nano-silver [33]	8.51	–	60 μg/m ³ Hg ⁰	20
S-activated carbon	2.6	–	Hg ⁰	
Micro-Se (commercial)	> 5.0	–		

Table 3
The special surface aeration of sample.

Sorbent	BET surface area (m ² /g)	Total pore volume (cm ³ /g)	Average pore diameter (nm)
CuS	31.129	0.153	17.918

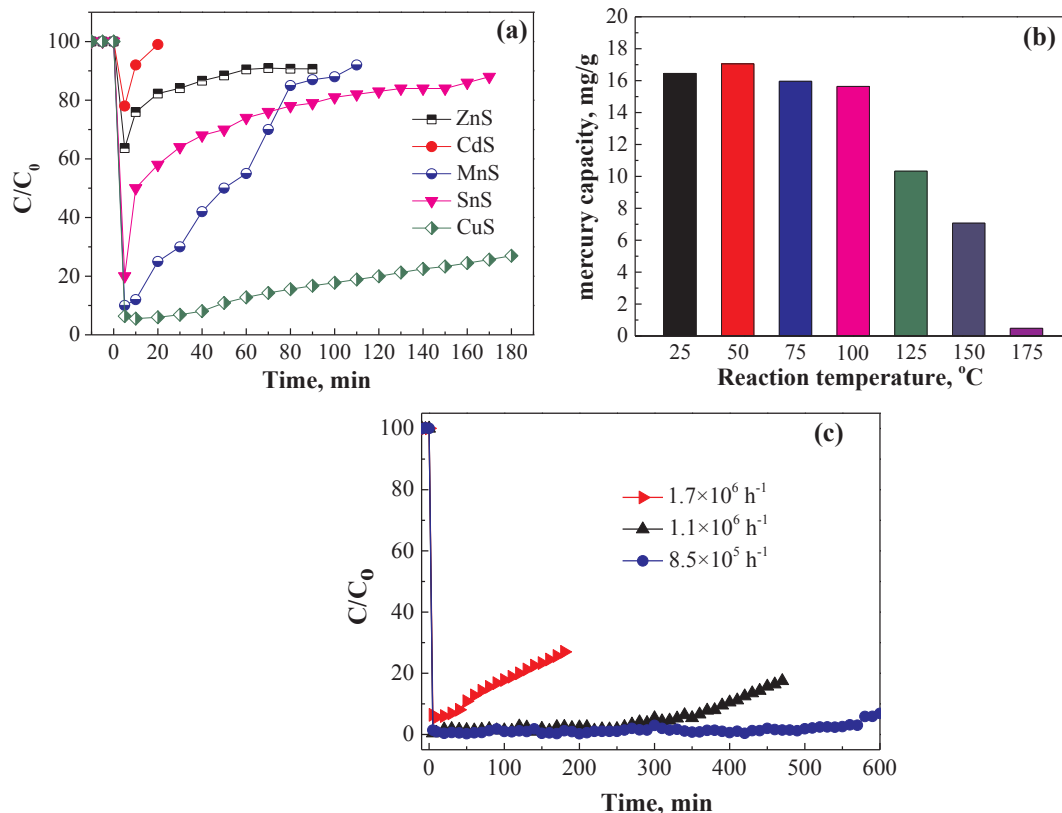


Fig. 3. Mercury removal performance of metal sulfides. (a) The Hg⁰ removal efficiency of different metal sulfides; (b) The effect of reaction temperature over CuS; (c) The effect of space velocities over CuS. Reaction conditions: 5% O₂ and 1300 μg/m³ Hg⁰ with 800 mL/min flow rate.

3.2. Elemental mercury removal performances of CuS

The experiments of different metal sulfides on Hg⁰ removal were tested at 50 °C. As shown in Fig. 3(a), these sorbents exhibited different performances. The efficiency order of the different metal sulfides could be expressed as follows: CuS > MnS > SnS > ZnS > CdS. CdS had nearly no Hg⁰ removal efficiency. The Hg⁰ removal efficiency of ZnS was lower than 40%. CuS had the best removal efficiency among these prepared materials. The Hg⁰ removal efficiency of CuS was about 70% after 3 h reaction. MnS and SnS could also adsorb a certain amount of mercury. While, their efficiencies were much lower than that of pure CuS. This indicated that the Cu-terminated active sites played a critical role in mercury adsorption.

The Hg⁰ removal performances over CuS at a temperatures range of 25–175 °C is presented in Fig. 3 (b). The mercury adsorption capacities at 25, 50, 75, 100, 125, 150, 175 °C for 180 min were 16.45, 17.05, 15.96, 15.64, 10.33, 7.07 and 0.48 mg/g, respectively. It was obvious that CuS exhibited optimal performance for Hg⁰ capture at 50 °C. The mercury adsorption capacities of CuS were similar to that range of 25–100 °C. With the increase of temperature from 125 to 175 °C, the mercury adsorption capacity decreased from 10.33 to 0.48 mg/g. The temperature of the downstream WFGS is generally lower than 75 °C. Therefore, low temperature (25–75 °C) was more suitable for Hg⁰ uptake over CuS in non-ferrous metal smelting flue gas. The mercury adsorption breakthrough curve over CuS was evaluated (shown in Fig.

S1). The adsorption rate of CuS for Hg⁰ capture at 50 °C was 0.0716 mg/(g·min) and its adsorption capacity was as high as 50.17 mg/g in the present of 5% O₂ (50% of the breakthrough threshold), which was much higher than those of sulfur modified activated carbon, micro-Se and metal sulfide listed in Table 2.

Supplementary data associated with this article can be found, in the

online version, at <https://doi.org/10.1016/j.fuel.2018.08.062>.

The Hg⁰ removal efficiencies under different space velocity were investigated by adjusting the amount of sorbents (10 mg, 15 mg, 20 mg). Fig. 3(c) shows the effect of space velocity on Hg⁰ removal over CuS. The Hg⁰ removal efficiency increased with the decreasing of space velocity. The initially efficiency was 94% at the space velocity of 1,700,000 h⁻¹ and decreased very quickly. When the space velocity decreased to 1,100,000 h⁻¹, the initially efficiency was 97.5% and remained for 160 min. The highest removal efficiency was nearly 100% under the space velocity of 850,000 h⁻¹ and almost kept constant until 570 min later. The space velocity used in this study was much higher than that in actual adsorption system. The lower the space velocity, the better Hg⁰ removal performance has over CuS. Therefore, CuS can still achieve higher Hg⁰ removal efficiency at 50 °C under the actual space velocity in the practical application.

3.3. Effects of flue gas components

According to the composition of the real non-ferrous smelting flue gas, we investigated the effects of gases such as O₂, H₂O, SO₂ and SO₃ on Hg⁰ removal at 50 °C and the results are summarized in Fig. 4.

The mercury adsorption capacity over CuS in the absence of O₂ was about 17.53 mg/g after 3 h reaction. When 5% and 10% O₂ were introduced into the simulated flue gas, the mercury adsorption capacities were 17.05 and 17.22 mg/g, respectively. This indicated that the

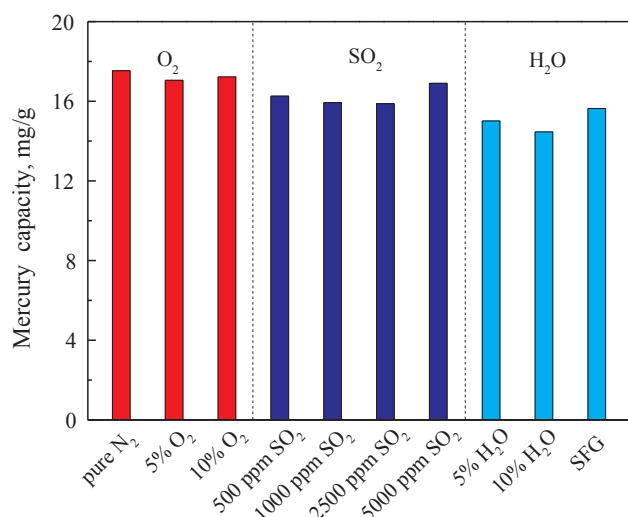


Fig. 4. Effects of flue gas components on Hg⁰ removal performance over CuS. Reaction conditions: ~1300 µg/m³ Hg⁰, GHSV = 1,700,000 h⁻¹, T = 50 °C, the adsorption time was 3 h.

presence of O₂ had little impact on Hg⁰ capture over CuS.

Traditional adsorbents like active carbon or transition metal oxide are inactivated for high concentration SO₂. The effect of SO₂ on Hg⁰ removal was also investigated under 5% O₂. As shown in Fig. 4, the mercury adsorption capacity was 15.05 mg/g in the absence of SO₂. When 500, 1000 and 2500 ppm SO₂ were introduced into the flue gas, the mercury adsorption capacities were 16.26, 15.93 and 15.88 mg/g, respectively. The mercury adsorption capacity was only slightly decreased under SO₂. When the concentration of SO₂ was increased to 5000 ppm, the mercury adsorption capacity was 16.9 mg/g. Results showed that SO₂ did not have a significant poison effect on mercury adsorption capacity. Therefore, CuS can capture gaseous Hg⁰ effectively under low or high concentration of SO₂.

H₂O vapor, as an inevitable component of flue gas, is considered to cause a negative effect on mercury removal over various adsorbents. The selenium filter, as one of specific adsorbents, has been used in non-ferrous metal smelter. However, it will quickly become ineffective and cannot regenerate, when H₂O vapor in the flue gas condenses. Thus, the effect of H₂O on Hg⁰ removal were studied. As shown in Fig. 4, the presence of H₂O had no obvious inhibition effect on Hg⁰ removal. Without H₂O, the mercury adsorption capacity in 3 h was 17.05 mg/g. when 5% and 10% H₂O was introduced into the flue gas, the mercury adsorption capacity seemed lower but it still maintained 15.01 and 14.46 mg/g, respectively. Large amount of SO₂ and H₂O vapor co-exist in the flue gas downstream the WFGS. Therefore, Hg⁰ removal under the stimulated flue gas condition (5% O₂, 10% H₂O, 1000 ppm SO₂) was investigated. Mercury adsorption capacity was slightly declined compared with that under 5% O₂.

Extensive studies have conducted to investigate the effects of flue gas compounds on Hg⁰ capture over sulfur-impregnated active carbon [17,23,24], metal oxides [14,25] and sulfides [19,20,26]. Sharon et al. found that the present of 10.7 ppm SO₃ could decrease mercury capture by activated carbon dramatically [27]. However, few literatures reported the effect of SO₃ on Hg⁰ removal over mineral sulfides. The concentration of SO₃ can reach up to 0.3 vol% in some zinc or copper smelter. In this work, SO₃-pretreated CuS was employed for Hg⁰ removal under an atmosphere of 5% O₂ at 50 °C to identify the possible surface deactivation by SO₃. Before the experiment, virgin CuS was first pretreated under a flow of 5% O₂ and 1000 ppm SO₃ with 800 mL/min for 1 h at 50 °C. As shown in Fig. 5, SO₃ exhibited a noticeable inhibitory effect on Hg⁰ adsorption. The efficiency of the SO₃-pretreated CuS gradually decreased to 40% after 180 min reaction, which was

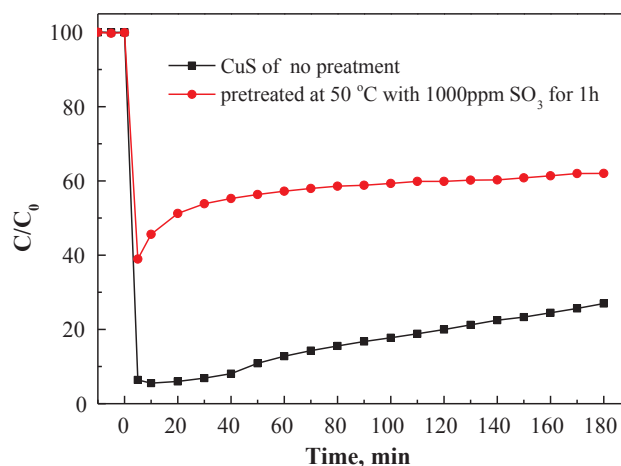


Fig. 5. Hg⁰ breakthrough curves of SO₃-pretreated CuS under 5% O₂ atmosphere.

much lower than that observed over CuS with no pretreatment. This indicated that the active surface Hg⁰ adsorption sites were at least partially destroyed or decreased during the SO₃ pretreatment process.

In conclusion, most of flue gas component had a negligible effect on Hg⁰ adsorption over CuS. And this is a tremendous advantage for removing Hg⁰ from non-ferrous metal smelting flue gas. Considering the toxicity of SO₃ to the sorbents and optimal reaction temperature, CuS can be injected between the WFGS and ESD systems for efficient Hg⁰ capture, where the acid mist has been basically cleared.

3.4. Hg⁰ adsorption mechanism over CuS

XPS analysis was adopted to determine the chemical state and the relative portion of main elements on the surface of samples. The XPS analysis of Cu 2p, O 1s, S 2p and Hg 4f for the fresh and used CuS under different gas conditions are showed in Fig. 6. The XPS spectrum of Cu in the 2p region for fresh CuS (Fig. 6(a)) shows the binding energies of Cu 2p_{3/2} and Cu 2p_{1/2} peaks at 932.5 and 952.4 eV, respectively, which were typical values for Cu²⁺ in CuS. However, after Hg⁰ adsorption, the XPS spectrum of CuS exhibited change. The binding energies of Cu 2p_{3/2} and Cu 2p_{1/2} slightly right-shift to lower binding energy, indicating the presence of either Cu⁰ or Cu⁺. This indicated that Cu²⁺ was partially reduced during Hg⁰ adsorption process.

As shown in Fig. 6(c), (d), (e), the S 2p spectra over the fresh and used CuS appeared at 162.2, 163.2 and 169.1 eV, which were attributed to S²⁻, S₂²⁻ and SO₄²⁻, respectively [18,20,26]. Three peaks for S appeared at the same peak position, indicated the sulfur species did not change after the reaction. As shown in Fig. 6(g, h), the obvious peaks of Hg 4f spectra over used CuS centered at 100.9 and 104.9 eV were assigned to surface HgS. As illustrated in the Table S1, the ratio of S₂²⁻ was decreased from 63.30 to 54.73% after adsorbing Hg⁰ in 5% O₂. Meanwhile, the ratio of S²⁻ was increased from 13.19 to 20.61%, which indicated that part of S₂²⁻ combined with mercury to form S²⁻. After adsorbing Hg⁰ in 5% O₂ + 5000 ppm SO₂, the mass ratio of S₂²⁻ was decreased from 63.30 to 47.48% compared with that under the atmosphere without SO₂. And the mass ratio of SO₄²⁻ was increased 3.25% compared with that under the atmosphere without SO₂. This suggested that S₂²⁻ played a key role in Hg⁰ capture by CuS.

According to the above discussion, both Cu and S active sites were responsible for Hg⁰ adsorption over CuS. Hg⁰ adsorption over CuS was followed the Mars-Maessen mechanism, and could be deduced as follows: firstly, gaseous Hg⁰ was adsorbed on the surface of CuS, forming Hg(ad). Then, Cu²⁺ and S₂²⁻ reacted with Hg(ad) to form HgS on its surface. And the reaction can be described as follows:

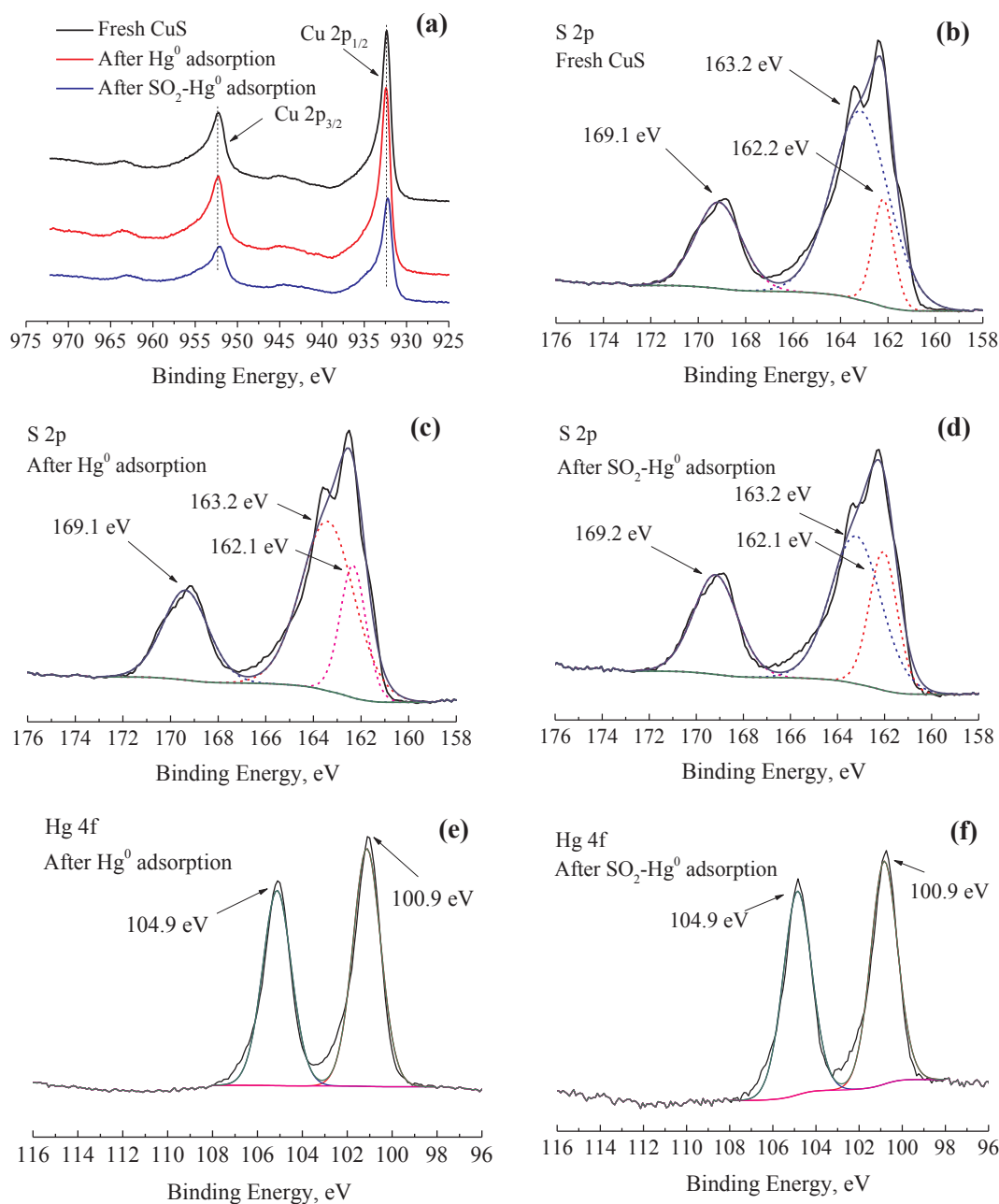


Fig. 6. XPS spectra: (a) Cu 2p of fresh and used CuS (b) S 2p of fresh CuS (c) S 2p of used CuS under Hg^0 atmosphere (d) S 2p of used CuS under $\text{SO}_2\text{-Hg}^0$ atmosphere (e) Hg 4f of used CuS under Hg^0 atmosphere (f) Hg 4f of used CuS under $\text{SO}_2\text{-Hg}^0$ atmosphere.



Hg-temperature programmed desorption (Hg-TPD) is an available approach to identify the mercury species [28]. Mercury species can be identified from the high peak temperature at which they are released. After Hg^0 adsorption under 5% O_2 , the sorbents were passed using pure N_2 at a heating rate $2^\circ\text{C}/\text{min}$ from 50 to 700°C . From Fig. 7, it was obvious that mercury desorbed during 100 to 240°C , with a peak at 215°C for used CuS with no pretreatment. This indicated that the primary mercury species was HgS black [26]. The CuS pretreated by SO_3 was also detected by TPD experiment. The CuS pretreated by SO_3 had four peaks at 135, 215, 350 and 615°C , respectively. The first peak at

the temperature of 135°C was desorption of Hg^0 . This demonstrated the binding affinity between sulfur site and Hg^0 was decreased, which might be because SO_3 was adsorbed on the surface of sorbents, and competed for the active sites of Hg^0 [24]. It indicated that the active surface Hg^0 adsorption sites were at least partially destroyed during the SO_3 pretreatment process. The second peak at the temperature of 210°C was HgS-black, and a broad peak was observed at the temperature range from 270 to 500°C , which was HgS-red [29,30]. The peak at approximately 615°C might be HgSO_4 [31]. These results were coincided fully with those shown in Fig. 5 that SO_3 evidently limited Hg^0 adsorption by CuS.

3.5. Procedure for mercury capture from non-ferrous flue gas

Fig. 8 shows a diagram of the recycle of CuS for mercury recovery from non-ferrous metal smelting flue gas as a cobenefit of the ESD. CuS

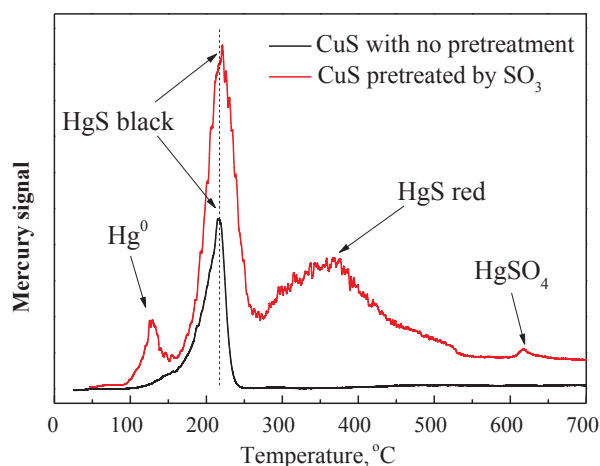


Fig. 7. TPD spectra of CuS used for Hg^0 adsorption at a heating rate of $2^\circ\text{C}/\text{min}$.

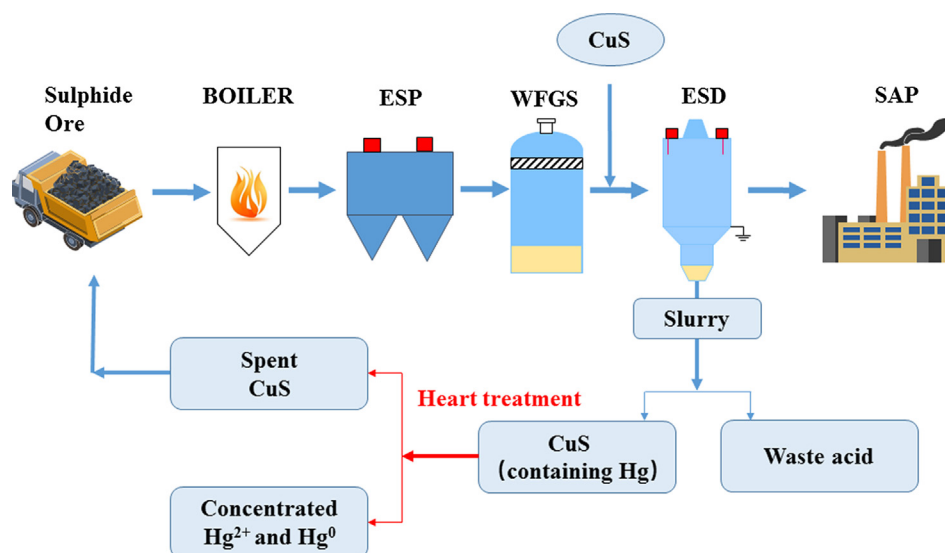


Fig. 8. Illustration of the recycle of CuS for mercury recovery from non-ferrous metal smelting flue gas as a co-benefit of the ESD.

powders will be injected into the flue gas downstream of the WFGS to capture Hg^0 . The temperature of the flue gas downstream WFGS is generally $35\text{--}50^\circ\text{C}$, and CuS shows an excellent performance for Hg^0 capture in this temperature range. Moreover, most of the SO_3 has been washed down by the WFGS. The effect of SO_3 on mercury adsorption can be ignored. After Hg^0 capture, CuS containing Hg will be collected by the ESD as a mixture with waste acid. CuS can be easily separated by conventional solid-liquid separation method like filtrate and precipitate. High concentrations of gaseous Hg^0 and Hg^{2+} will be released from the spent CuS by the thermal treatment at 250°C . High concentrations of gaseous Hg are easily recovered for centralized control. Deactivated CuS will be transferred to the furnace to recover sulfur resources.

4. Conclusions

A series of metal sulfides were prepared to investigate Hg^0 removal performances from non-ferrous metal smelting flue gas. CuS presented a super mercury adsorption capacity (50.17 mg/g with the 50% breakthrough threshold at 50°C) than the previous reported sorbents. There were no obvious poison effects on Hg^0 removal in presence of SO_2 , H_2O and O_2 . However, SO_3 can compete mercury adsorption sites on CuS surface. Adequate surface coverage of S_2^{2-} and Cu^{2+} sites were critical

to Hg^0 adsorption, forming extremely stable mercuric sulfides (HgS) species on the sorbents surface. This research also provided a technical process for industrial application to recover Hg^0 from the flue gas as a co-benefit of ESD. The sorbents can be injected into upstream of ESD, where SO_3 has been almost removed completely and gas temperature is about 50°C . Future work needs to further improve mercury adsorption capacity of CuS and develop other metal sulfides. Moreover, the influence mechanism of SO_3 on the mercury adsorption will be studied as well.

Acknowledgments

This study was supported by the National Key R&D Program of China (2017YFC0210500) and the National Natural Science Foundation of China (No. 51478261 and No. 21677096). This study was also supported by National Postdoctoral Program for Innovative Talents (No. BX201700151). Thanks for the support of China's Post-doctoral Science Fun (No. 2017M620156).

References

- [1] Clarkson TW, Magos L. The toxicology of mercury and its chemical compounds. *Crit Rev Toxicol* 2006;36(8):609–62.
- [2] Lin Y, Wang S, Steindal EH, Wang Z, Braaten HF, Wu Q, et al. A holistic perspective is needed to ensure success of minamata convention on mercury. *Environ Sci Technol* 2017;51(3):1070–1.
- [3] Wu Q, Wang S, Hui M, Wang F, Zhang L, Duan L, et al. New insight into atmospheric mercury emissions from zinc smelters using mass flow analysis. *Environ Sci Technol* 2015;49(6):3532–9.
- [4] Zhang L, Wang S, Wang L, Wu Y, Duan L, Wu Q, et al. Updated emission inventories for speciated atmospheric mercury from anthropogenic sources in China. *Environ Sci Technol* 2015;49(5):3185–94.
- [5] Streets DG, Horowitz HM, Jacob DJ, Lu Z, Levin L, Ter Schure AFH, et al. Total mercury released to the environment by human activities. *Environ Sci Technol* 2017;51(11):5969–77.
- [6] Lin Y, Wang S, Steindal EH, Zhang H, Zhong H, Tong Y, et al. Minamata convention on mercury: Chinese progress and perspectives. *Natl Sci Rev* 2017;4(5):677–9.
- [7] Zhang L, Wang S, Wu Q, Wang F, Lin C-J, Zhang L, et al. Mercury transformation and speciation in flue gases from anthropogenic emission sources: a critical review. *Atmos Chem Phys* 2016;16(4):2417–33.
- [8] Liu Z, Peng B, Chai L, Liu H, Yang S, Yang B, et al. Selective removal of elemental mercury from high-concentration SO_2 flue gas by thiourea solution and investigation of mechanism. *Ind Eng Chem Res* 2017;56(15):4281–7.
- [9] Habashi F. Metallurgical plants: how mercury pollution is abated. *Environ Sci Technol* 1978;12(13):1372–6.
- [10] Hylander LD, Herbert RB. Global emission and production of mercury during the pyrometallurgical extraction of nonferrous sulfide ores. *Environ Sci Technol* 2008;42(16):5971.

- [11] Ralston N. Nano-selenium captures mercury. *Nat Nanotechnol* 2008;3(11):648.
- [12] Hamzehlouyan T, Sampara C, Li J, Kumar A, Epling W. Experimental and kinetic study of SO₂ oxidation on a Pt/γ-Al₂O₃ catalyst. *Appl Catal B* 2014;152–153:108–16.
- [13] Zhou Q, Duan Y-F, Hong Y-G, Zhu C, She M, Zhang J, et al. Experimental and kinetic studies of gas-phase mercury adsorption by raw and bromine modified activated carbon. *Fuel Process Technol* 2015;134:325–32.
- [14] Zou S, Liao Y, Xiong S, Huang N, Geng Y, Yang S. H₂S-modified Fe-Ti spinel: a recyclable magnetic sorbent for recovering gaseous elemental mercury from flue gas as a co-benefit of wet electrostatic precipitators. *Environ Sci Technol* 2017;51(6):3426–34.
- [15] Yang S, Liu C, Liu Z, Yang B, Xiang K, Zhang C, et al. High catalytic activity and SO₂-poisoning resistance of Pd/CuCl₂/γ-Al₂O₃ catalyst for elemental mercury oxidation. *Catal Commun* 2018;105:1–5.
- [16] Ma J, Li C, Zhao L, Zhang J, Song J, Zeng G, et al. Study on removal of elemental mercury from simulated flue gas over activated coke treated by acid. *Appl Surf Sci* 2015;329:292–300.
- [17] Liu W, Vidic RD, Brown TD. Impact of flue gas conditions on mercury uptake by sulfur-impregnated activated carbon. *Environ Sci Technol* 2000;34(34):154–9.
- [18] Li H, Zhu L, Wang J, Li L, Shih K. Development of nano-sulfide sorbent for efficient removal of elemental mercury from coal combustion fuel gas. *Environ Sci Technol* 2016;50(17):9551–7.
- [19] Li H, Zhu L, Wang J, Li L, Lee PH, Feng Y, et al. Effect of nitrogen oxides on elemental mercury removal by nanosized mineral sulfide. *Environ Sci Technol* 2017;51(15):8530–6.
- [20] Liao Y, Chen D, Zou S, Xiong S, Xiao X, Dang H, et al. Recyclable naturally derived magnetic pyrrhotite for elemental mercury recovery from flue gas. *Environ Sci Technol* 2016;50(19):10562–9.
- [21] Xiang W, Liu J, Chang M, Zheng C. The adsorption mechanism of elemental mercury on CuO (110) surface. *Chem Eng J* 2012;200–202:91–6.
- [22] Li F, Wu J, Qin Q, Li Z, Huang X. Controllable synthesis, optical and photocatalytic properties of CuS nanomaterials with hierarchical structures. *Powder Technol* 2010;198(2):267–74.
- [23] Mitsui Y, Imada N, Kikkawa H, Katagawa A. Study of Hg and SO₃ behavior in flue gas of oxy-fuel combustion system. *Int J Greenhouse Gas Control* 2011;5:S143–50.
- [24] He P, Wu J, Jiang X, Pan W, Ren J. Effect of SO₃ on elemental mercury adsorption on a carbonaceous surface. *Appl Surf Sci* 2012;258(22):8853–60.
- [25] Yang Y, Liu J, Zhang B, Zhao Y, Chen X, Shen F. Experimental and theoretical studies of mercury oxidation over CeO₂–WO₃/TiO₂ catalysts in coal-fired flue gas. *Chem Eng J* 2017;317:758–65.
- [26] Xu H, Yuan Y, Liao Y, Xie J, Qu Z, Shangguan W, et al. [MoS₄](2-) cluster bridges in Co-Fe layered double hydroxides for mercury uptake from S-Hg mixed flue gas. *Environ Sci Technol* 2017;51(17):10109–16.
- [27] Sjoström S, Dillon M, Donnelly B, Bustard J, Filippelli G, Glesmann R, et al. Influence of SO₃ on mercury removal with activated carbon: Full-scale results. *Fuel Process Technol* 2009;90(11):1419–23.
- [28] Xu H, Ma Y, Huang W, Mei J, Zhao S, Qu Z, et al. Stabilization of mercury over Mn-based oxides: speciation and reactivity by temperature programmed desorption analysis. *J Hazard Mater* 2017;321:745–52.
- [29] Rumayor M, Lopez-Anton MA, Diaz-Somoano M, Maroto-Valer MM, Richard JH, Biester H, et al. A comparison of devices using thermal desorption for mercury speciation in solids. *Talanta* 2016;150:272–7.
- [30] Homayoon F, Faghihian H, Torki F. Application of a novel magnetic carbon nanotube adsorbent for removal of mercury from aqueous solutions. *Environ Sci Pollut Res Int* 2017;24(12):11764–78.
- [31] Rumayor M, Diaz-Somoano M, Lopez-Anton MA, Martinez-Tarazona MR. Mercury compounds characterization by thermal desorption. *Talanta* 2013;114:318–22.
- [32] Liao Y, Xia Y, Zou S, Liu P, Liang X, Yang S. In situ emergency disposal of liquid mercury leakage by Fe-containing sphalerite: performance and reaction mechanism. *Ind Eng Chem Res* 2016;56(1):153–60.
- [33] Johnson NC, Manchester S, Sarin L, Gao Y, Kulaots I, Hurt RH. Mercury vapor release from broken compact fluorescent lamps and in situ capture by new nanomaterial sorbents. *Environ Sci Technol* 2008;42(15):5772–8.